MADRID
inter.noise 2019
June 16 - 19
NOISE CONTROL FOR A BETTER ENVIRONMENT

# Numerical modelling and characterization of a heat exchanger

**G. Vatin, B. Ganty, Y. Detandt[1]**
**Free Field Technologies, MSC Software Belgium**
**9 rue Emile Francqui, B-1435 Mont-Saint-Guibert, Belgium**

**S. Lesoinne, J.-J. Embrechts[2]**
**Acoustics Laboratory, University of Liège**
**Quartier Polytech 1, 10 Allée de la découverte, B-4000 Liège, Belgium**

## ABSTRACT

**Strong insulation in modern building and housing requires efficient ventilation systems. A popular solution is a decentralized set-up with one ventilation unit per room. The noise emitted by a ventilation unit then has a major impact on the room comfort. In order to reduce the heat transfer to the outside, a ventilation unit is typically designed as a double flux-system with a heat exchanger. This exchanger has a noticeable impact on the acoustic behavior of the ventilation unit. It is therefore of interest to study its effect through numerical simulations. The numerical modelling of a realistic heat exchanger is presented in this paper. The exchanger is placed inside its ventilation casing and modelled using a double equivalent fluid homogenization. Unknown homogenization properties are retrieved in two steps. Acoustic transfer functions are first measured experimentally in order to characterize the propagation paths through the heat exchanger. In a second step, an optimization loop is computed with the numerical model of the heat exchanger. This allows to determine the homogenization properties fitting the measured transfer functions for each frequency. Finally the results for the characterized heat exchanger homogenization model are compared against measurement.**

**Classification of Subjects.**
**Keywords: HVAC noise, Heat exhanger, Ventilation noise, Noise simulations,**
**I-INCE Classification of Subject Number: 30**

[1] Corresponding author : guillaume.vatin@fft.be

[2] Corresponding author : jjembrechts@uliege.be

# 1. INTRODUCTION

Todays new standards in buildings require eco-friendly ventilation systems delivering fresh air in quiescent places. The noise level emitted by these ventilation systems is therefore a key point in the selection of the system. The present paper investigates the noise emitted by a decentralized system. As the noisy devices (fans) are located directly in the quiet places (bedrooms, …) a special care should be taken to design and select the quietest fans on the market while checking the acoustic interaction effects of the additional components of the system (heat exchanger, casing, …). In a double-flux system, two fans operate at the same time, enforcing the expected air flow rate of fresh and waste air. Figure 1 shows a schematic view of a double flux system.

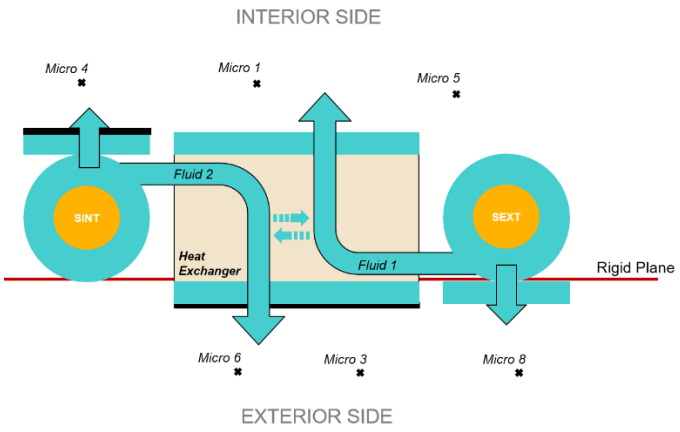


*Figure 1 - Schematic View of the heat exchanger*

The heat exchanger component is part of the air flow system, possibly participating to the acoustic damping of the noise emitted by the fan if located downstream. This needs to be assessed by measurements (section 2) and numerical investigations (section 3) for future design and optimisation of the module. For numerical efficiency, all the channels of the heat exchanger are not discretized, but replaced by a numerical model including the visco-thermal effects. While most of the acoustic parameters of this model are derived from geometrical properties, some are related to material damping properties in a complex manner. These last parameters have been calibrated by means of specific measurements which are presented in section 2. Based on these measurements, the numerical acoustic models are calibrated. The numerical solutions provides a better insight of the heat exchanger acoustic performances.

# 2. EXPERIMENTAL ANALYSIS

## 2.1 Experimental set-up

The ventilation unit is equipped with two fans: one extracts the air from the interior side of the building and the other one feeds the room with fresh air. For the measurement of acoustic transfer functions, each fan is replaced in the unit by a small loudspeaker. The acoustic impulse responses (IR) are then measured between each source position and several microphone positions defined close to the apertures of the unit's envelope (air inputs and outputs).

The impulse responses have been measured in the anechoic room of the Acoustics laboratory of the University of Liège, in order to avoid the influence of room reverberation on the results. The ventilation module has been inserted into a big baffle (2.44m x 2.44m), composed of two MDF plates: see Figure 2 (a). The front panel of the module has been removed on the interior side, in order to have a direct access to the air extraction and blowing apertures.

The use of a baffle is justified by the necessity to simulate the real-case scenario in which the ventilation unit is embedded into a wall. The baffle should (as far as possible) attenuate the diffraction of the sound waves transmitted from the exterior apertures to the interior side. According to usual practice in loudspeakers' frequency response measurements, the centre of the acoustic source should be located in an asymmetric position related to the baffle rectangular area [1]. In this case, as there are several apertures in the module for air inlet and outlet, a compromise had to be found for its final position into the baffle. The waste air inlet has been considered as the main acoustic source on the interior side and, therefore, its central position is slightly asymmetric in height and width. As a consequence, the choice of this particular position also resulted in an asymmetric position of the fresh air inlet on the exterior side of the module.

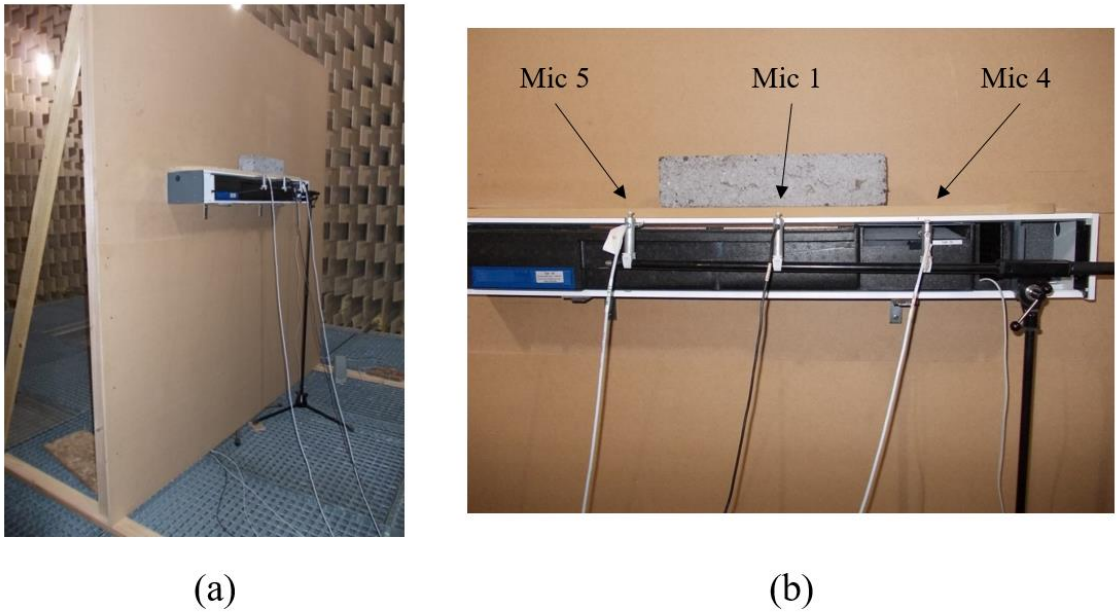


*Figure 2: (a) The ventilation module and its baffle in the anechoic room (interior side) – (b) Front face of the module with the three interior microphones*

A 2" loudspeaker has been chosen as the acoustic source (Visaton FRS 5 XWP – 8 ohms, 5W) connected to a 2x5W audio amplifier. The loudspeaker has been positioned at the centre of the circular fan cavity, through a flexible connection with the module in order to attenuate the vibrations directly transmitted by the loudspeaker to module structure.

The two fans have been removed during the measurements: only one fan cavity is occupied by the loudspeaker, the other cavity being empty. The two anti-dust filters were always present.

Six microphones are located at fixed and well-defined positions, close to the apertures for air inlet/outlet. Figure 2 (b) shows the 'front' or 'interior' face of the ventilation module and the three interior microphones.

## 2.2 Measurement configurations

For each of the two loudspeaker positions, five configurations are defined. In a given configuration, some air apertures are blocked and some others are left open, in order to characterize different sound propagation paths. The apertures are alternatively blocked with small wood panels adapted to their size, except for the air outlet aperture situated on the exterior side which has been filled with mastic gum.

The five configurations with the loudspeaker in the fan cavity extracting interior air are described in Table 1. Similar configurations have been defined for the other source position. For each configuration, six IRs are simultaneously measured at the microphone positions.

| Configurations | Interior air inlet | Air outlet – Interior side | Exterior air inlet | Air outlet – Exterior side | SINT | SEXT |
|---|---|---|---|---|---|---|
| 1/2 | open | close | open/close | close/open | ON | OFF |
| 3/4 | close | open | open/close | close/open | ON | OFF |
| 9 | close | close | close | close | ON | OFF |

*Table 1 - Five measurement configurations with SINT 'on'. 'SINT' means that the source (loudspeaker) is in the fan cavity extracting interior air. 'SEXT' means that the source is in the other cavity*

## 2.3 Measurement results

The signal feeding the loudspeaker is a logarithmic sine sweep having a duration of 1second (in fact, three sweeps of 1s are emitted between the frequencies 50Hz and 22000Hz, separated by a silence of 1s). The sampling frequency is 44.1 kHz. The microphone signals are all recorded and de-convolved to obtain the impulse response [2]. The level of the signal is kept constant for all the IR measurements.

Signal processing starts with the extraction of the 'linear part' of the impulse response: for more information about IR measurements with logarithmic sine sweeps, see [2]. Approximately 10000 samples of each linear IR are extracted (~0.23s @ FS=44100 Hz). Then, the Fourier transform is applied to obtain the acoustic transfer function between 0 and 22050 Hz (resolution 4.4 Hz). As an example, Figure 3 shows the acoustic transfer functions measured at microphone number 4. In these configurations, the loudspeaker is in the fan cavity situated just in front of this microphone.

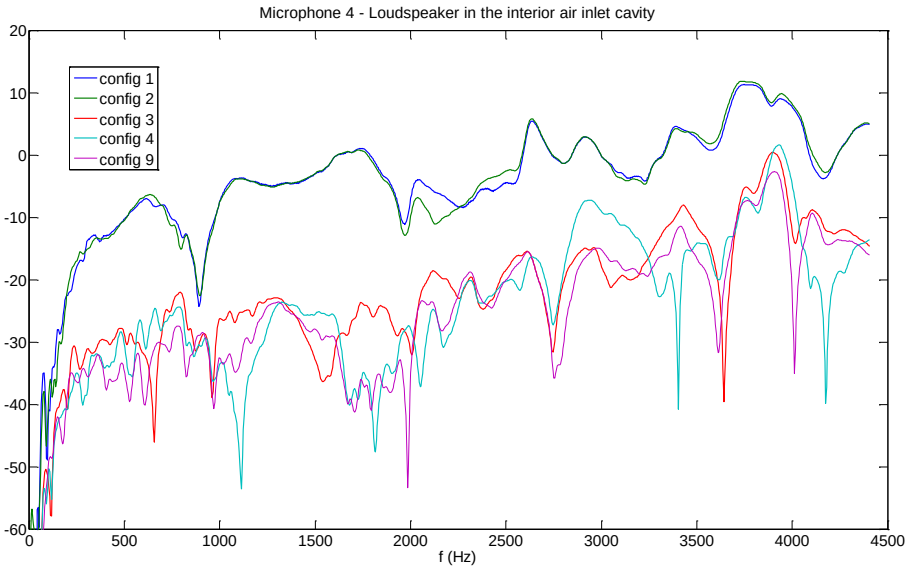


*Figure 3 - Acoustic transfer functions (amplitude) measured at microphone number 4, in the five configurations with the loudspeaker in the SINT position*

In configurations 1 and 2, the aperture in front of the microphone number 4 is open (blue and green curves). The contribution of SINT is therefore maximal in those configurations, and very similar whatever if the exterior apertures are open or close. On the contrary, the interior fresh air aperture (open in configurations 3 and 4) does not bring significant acoustic pressure at microphone 4, approximately 10 to 20 dB less than the air inlet aperture, depending on frequency (red and light blue curves). Finally, configuration 9 which corresponds to all apertures closed gives the lowest contribution at almost all frequencies, except for some negative interferences in configuration 4. From this analysis, one can conclude that configurations 1 and 2 curves in Figure 4 give the transfer function of the propagation path between the fan cavity and the air inlet aperture.

Figure 4 shows the acoustic transfer functions measured at microphone number 5, the leftmost one in Figure 2(b). The difference between configurations 3 and 4 is the status (open/close) of the two apertures situated on the exterior side of the module. As both curves are very similar, these two apertures seem to have little influence (by diffraction) on microphone 5. However, the emergence of the two curves above ‘config 9’ (all apertures closed) is less than in the case of microphone 4: approximately 5 dB until 2000 Hz. Above this frequency, the response measured at microphone 5 contains other contributions than the aperture in front of it, especially coming from the vibrations of the casing and/or residues from other apertures. The same conclusion holds for microphone 1, above 2.5 kHz and also for the three other microphones located on the exterior side (not shown).

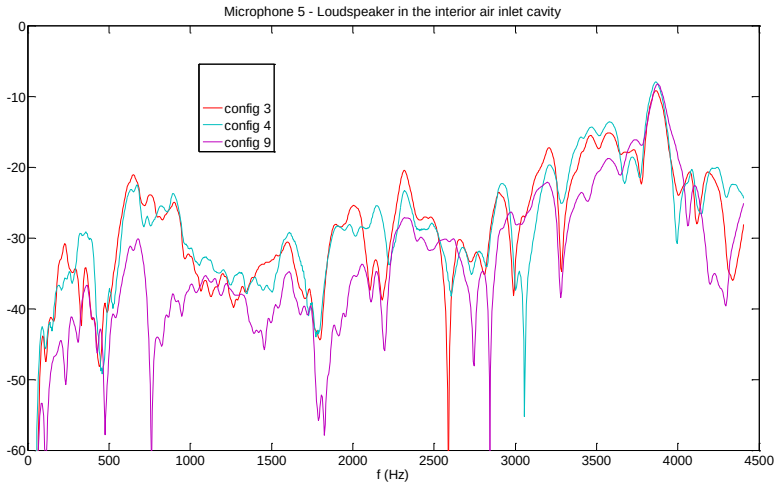


*Figure 4 - Acoustic transfer functions (amplitude) measured at microphone number 5, in three configurations, with the loudspeaker in the SINT position*

### 2.4 Frequency response of the loudspeaker and microphones

The acoustic transfer functions shown in Figure 3 and Figure 4 include the responses of the loudspeaker and the microphones. To extract these contributions, each pair of loudspeaker and microphone has been used in a frequency response measurement.

For these experiments, the ventilation module has been removed from the baffle and it was put on a support without the metallic casing, in another anechoic room. The upper plate has been removed such that the loudspeaker was free to radiate in free field. The microphone was hanging 1 meter just above the centre of the membrane. The six microphones were successively positioned at the same location and the impulse responses were then measured, using the same logarithmic sweep method. These IRs have finally been used to calibrate the acoustic transfer functions previously shown.

## 3. ACOUSTIC SIMULATIONS

### 3.1 Introduction of the model

Acoustic simulations are performed using Actran, a finite element-based modelling software developed by Free Field Technologies. This section describes the numerical model baseline used for the heat exchanger characterization [3].

Starting from a CAD (Computer Aided Design), the air inside the module (Figure 5) and a part of the air around it (Figure 7) are meshed using quadratic tetrahedral elements

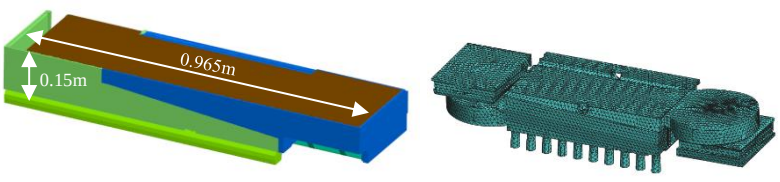


*Figure 5 - 3D CAD of module (left) interior mesh (right)*

The element size $h$ is chosen based a 6 elements per wavelength criteria. This results in $h = \frac{1}{6}\lambda \cong 0.01\ m$, with $\lambda$ as the minimal acoustic wavelength corresponding to the maximal frequency of the analysis (5000Hz).

Several parts are identified on the interior mesh as shown on Figure 6. The air extraction volumes are two separated acoustic domains for each flow paths. They are connected between each other through the heat exchanger.

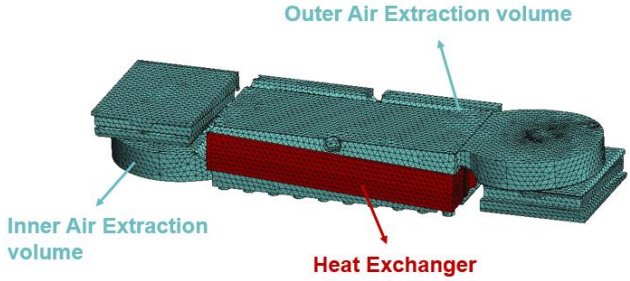


*Figure 6 - Part identification inside HVAC module*

As in experiments, fans are not included in the model. Filters are also no taken into account in the simulation as experiments show they can be considered as acoustically transparent. The acoustic excitation SINT or SEXT is represented by a spherical source (monopole), which allow to fix an acoustic pressure of 1Pa at 1 meter. Monopole is placed at the same location as loudspeaker in experiments. Walls of module are considered rigid, which means that acoustic waves are fully reflected on the interior air volume free faces. Near field of interior and exterior air is partially modelled. Non-reflecting boundary conditions are then applied to model semi-free fields around the air module (see Figure 7). As for the exchanger, it is modelled using a specific homogenization approach described in the next section.

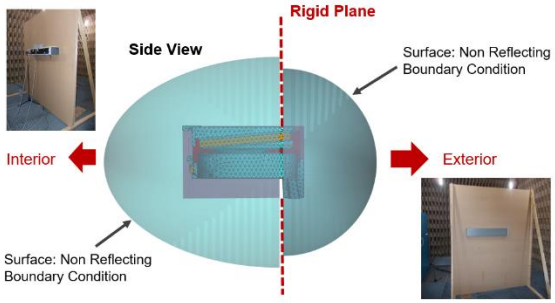


*Figure 7 - Numerical model which mimics experimental setup*

## 3.2 Theory for heat exchanger modelling

In the heat exchanger, two opposite channels rows have to be considered where air from inside and air from outside flows in counter-current (Figure 8).

The heat exchanger is made of thin plastic sheets. The two counter-current air fluxes are propagating on each sides of the sheets. The sheets are folded, therefore creating small channels where air fluxes can propagate.

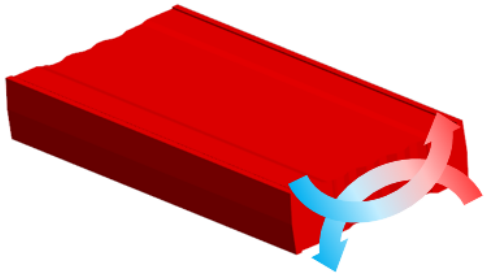

*Figure 8 - Counter-current flows in exchanger*

Viscous-thermal effect induced by these channels have a high impact on acoustic propagation. Inside thin fluid air layer close to rigid walls, fluid viscosity and its conductivity lead to a dissipation of acoustic energy. Acoustic waves are locally damped (Figure 9):

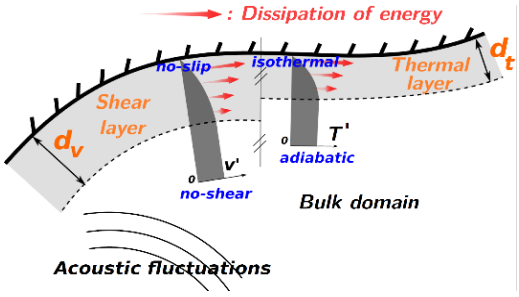


*Figure 9 - Viscous-thermal effects*

Modelling small channels with finite elements is not reasonable. Indeed, small elements should be defined which would severely increases number of degrees of freedom. Actran uses a homogenized formulation allowing to:

1. model narrow channels dissipation effects without representing the detailed geometry with finite elements.
2. model interactions between double-duct arrays and their effect on acoustic propagation.

Two numerical ingredients are used to build the homogenized model for double-duct arrays.

First, the eXtended Low Reduced Frequency (XLRF) is an extension of the LRF method (W. Beltman) [4][5] allows to model acoustic propagation accounting for viscous-thermal and convection effects (1). It relies on linearized Navier-Stokes equations in frequency domain, and split the coordinate system into propagation ($pd$) and cross ($xd$) directions (see Figure 10). Also, it considers plane wave propagation, which is a hypothesis valid for narrow channels or thin layers: $p(\boldsymbol{x}) = p(\boldsymbol{x}_{pd})e^{i\omega t}$.

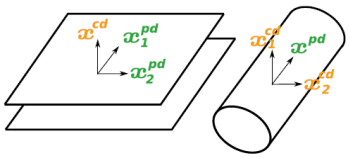


*Figure 10 - Coordinate system for duct model*

$$\boldsymbol{\nabla}.\left(\frac{\|\tilde{c}\|^2-\|\overline{\boldsymbol{v}}\|^2}{\tilde{\rho}}\boldsymbol{\nabla}\psi-i\omega\frac{\overline{\boldsymbol{v}}}{\tilde{\rho}\tilde{c}^2}\psi\right)-i\omega\frac{\overline{\boldsymbol{v}}}{\tilde{\rho}\tilde{c}^2}.\boldsymbol{\nabla}\psi+\frac{\omega^2}{\tilde{\rho}\tilde{c}^2}\psi=i\omega q+\boldsymbol{\nabla}\cdot(\overline{\boldsymbol{v}}q) \qquad (1)$$

With: density $\tilde{\rho}$, speed of sound $\tilde{c}$, mean flow velocity $\overline{\boldsymbol{v}}$, potential speed $\psi$, local volume source $q$.

The second ingredient is an anisotropic porous model, where the skeleton is assumed motionless. It allows to model an equivalent fluid with anisotropic properties which provides an anisotropic wave equation.

Combining the two numerical ingredients modifies the equation (1) into convected wave equation for one duct (2):

$$\boldsymbol{\nabla}.\left(\frac{\Omega\underline{\underline{\boldsymbol{A}}}(\|\tilde{c}\|^2-\|\overline{\boldsymbol{v}}\|^2)}{\tilde{\rho}\tilde{c}^2}\boldsymbol{\nabla}\psi-i\omega\frac{\Omega\overline{\boldsymbol{v}}}{\tilde{\rho}\tilde{c}^2}\psi\right)-i\omega\frac{\Omega\overline{\boldsymbol{v}}}{\tilde{\rho}\tilde{c}^2}.\boldsymbol{\nabla}\psi+\frac{\Omega\omega^2}{\tilde{\rho}\tilde{c}^2}\psi=i\omega q+\boldsymbol{\nabla}\cdot(\overline{\boldsymbol{v}}q) \qquad (2)$$

With the porosity $\Omega$ and orientation vector of duct $\underline{\underline{\boldsymbol{A}}}$.

Acoustic transfer between the two ducts are handled by a transfer admittance matrix where pressure $p$ and $q$ are coupled:

$$\begin{bmatrix}q_1\\q_2\end{bmatrix}=\begin{bmatrix}T_{11}&T_{12}\\T_{21}&T_{22}\end{bmatrix}\begin{bmatrix}p_1\\p_2\end{bmatrix} \qquad (3)$$

$$\begin{bmatrix} T_{11} & T_{12} \\ T_{21} & T_{22} \end{bmatrix} = \begin{bmatrix} \frac{1}{i\omega R} - \frac{1}{2K} & -\frac{1}{i\omega R} - \frac{1}{2K} \\ -\frac{1}{i\omega R} - \frac{1}{2K} & \frac{1}{i\omega R} - \frac{1}{2K} \end{bmatrix} \quad (4)$$

With $R$ the flow resistivity of the porous material, which will be characterized, and $K$ the bulk modulus.

These two ingredients allow a homogenized representation of any doubled duct system [6], accounting for the dissipation due to the acoustic propagation through narrow channels as well as the acoustic transfer between the two duct systems.

### 3.3 Heat exchanger characterization

The parameters necessary to model the heat exchanger as a homogenized component are the geometrical properties of the propagations ducts as well as the resistivity. The geometrical properties of the heat exchanger have been fixed reasonably based on the geometry of the sections of channels. The flow resistivity remains the unknown acoustic property to find. The real part of the resistivity can be interpreted as the resistance encountered by acoustic waves going from one channel to the neighbour channel. The imaginary part takes into account the fluid inertia and the wall stiffness which undergoes a deflection due to the pressure differential from each sides.

The method to determine the heat exchanger resistivity is based on a numerical model of the experimental set-up, which can be used to find the resistivity values leading to the same pressure values as the ones measured at the microphones. Thanks to an optimization loop, the resistivity is can be adjusted with the aim to fit numerical results with experimental results.

Among the experimental setups, the configuration 3 is chosen and reproduced numerically for the characterization because the acoustic waves are forced to propagate across the exchanger walls (see Figure 12). The resistivity of the exchanger can therefore be more easily evaluated. Acoustic source S_INT is a monopole.
Microphones are placed at same locations as in experimental setup, and results at microphones 1, 5 and 8 are used since they are placed in front of open outlets.

Acoustic Transfer Function (TF) is an acoustic response at a microphone induced by an excitation. TF of heat exchanger are computed numerically and compared with experiments. The optimization loop uses COBYLA algorithm (for Constrained Optimization BY Linear Approximations) from NLOPT and an objective function is set. This function (5) is defined as the sum of weighted square differences of transfer functions at each microphone:

$$f_{obj}(f) = \left[\frac{(TF_{Num1} - TF_{XP1})}{TF_{XP1}}\right]^2 + \left[\frac{(TF_{Num5} - TF_{XP5})}{TF_{XP5}}\right]^2 + 2\left[\frac{(TF_{Num8} - TF_{XP8})}{TF_{XP8}}\right]^2 \quad (5)$$

$TF_{Numi}$ *Numerical Transfer Function to microphone i*
$TF_{XPj}$ *Experimentl Transfer Function to microphone j*

*<u>Remark 1:</u> The acoustic transfer function of exchanger is defined as the ratio between transfer function of the whole system and the acoustic transfer function in straight propagation between source and a microphone at 1 meter.*
*<u>Remark 2:</u> A factor 2 is applied on microphone 8 from exterior side to balance due to the fact that we have two microphones on the interior side.*
*<u>Remark 3:</u> The algorithm COBYLA allows to quickly find the unknown parameter optimal value. It compares the objective function slope between each iteration. Knowing upper and lower limits of unknown parameter is mandatory to avoid local optimal value.*

### 3.4 Results

Results of optimization loop provides the real part and imaginary part of the frequency dependent flow resistivity of the exchanger. In spite of the fluctuating aspect, the flow resistivity is globally increasing with the frequency. This behaviour is observed in porous materials. Moreover, as this parameter is supposed to take into account other physical phenomena (fluid inertia and wall stiffness). Therefore, these frequency-dependant values are reasonable.

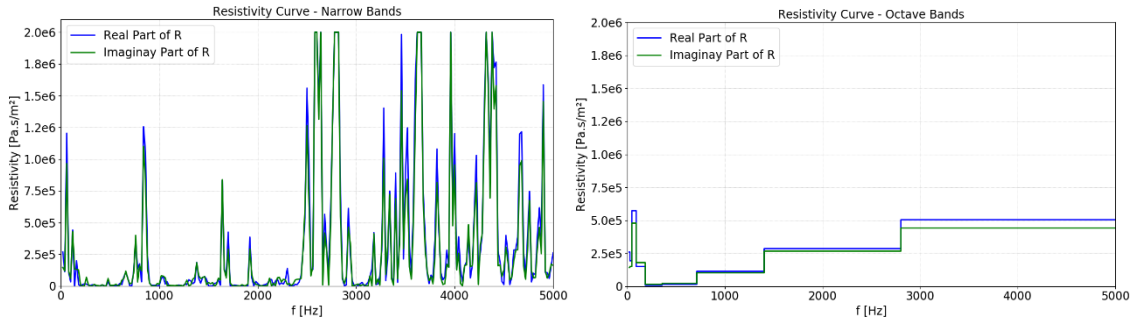


*Figure 11 - Flow resistivity found by optimization loop in narrow band (top) and octave band (bottom)*

The experimental acoustic transfer functions of the exchanger are then compared to the numerical transfer functions with resistivity found by optimization loop for the configurations 3 (see Figure 12). The comparison in-between the numerical and experimental transfer functions show a good correlation over the frequency range.

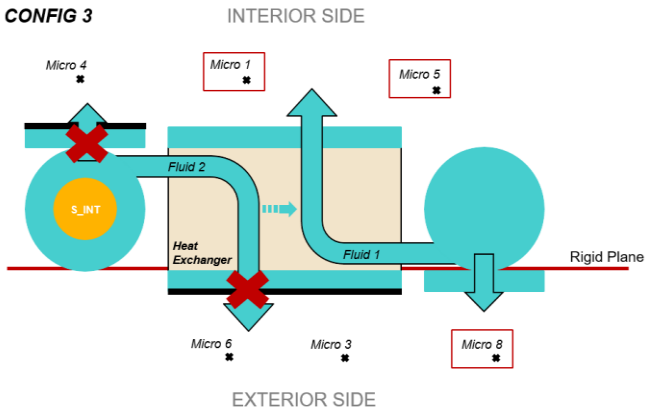


*Figure 12 - Simple scheme of acoustic waves paths in module – Configuration 3*

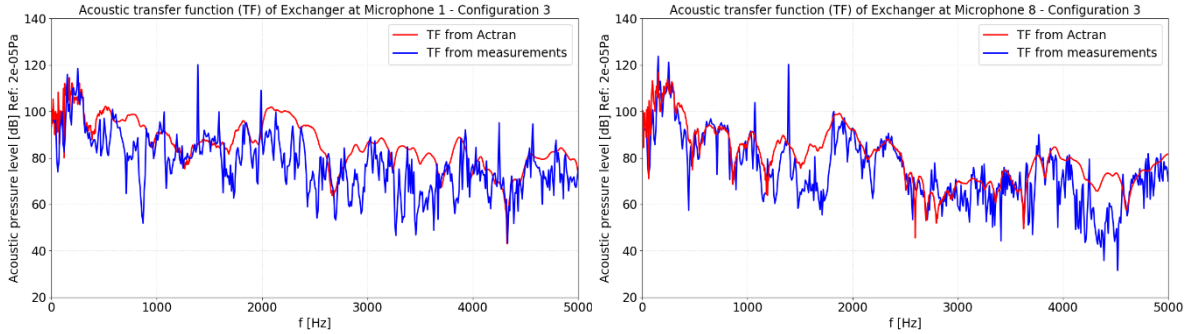


*Figure 13 - Acoustic transfer functions of exchanger with optimal Resistivity - Configuration 3*

To further validate the resistivity values, acoustic transfer functions are compared for an alternative configuration corresponding to a mirror of configuration 3, namely configuration 6 (Figure 14). Acoustic waves are also forced to propagate across the heat exchanger to go outside the ventilation unit.

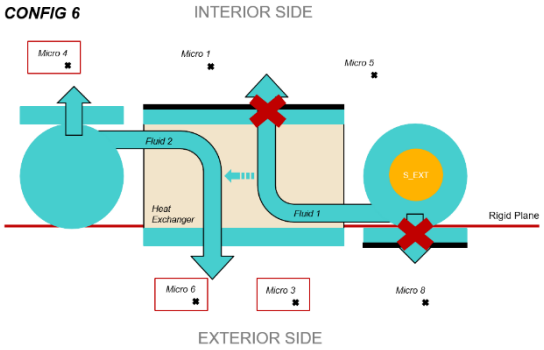


*Figure 14 - Simple scheme of acoustic waves paths in module – Configuration 6*

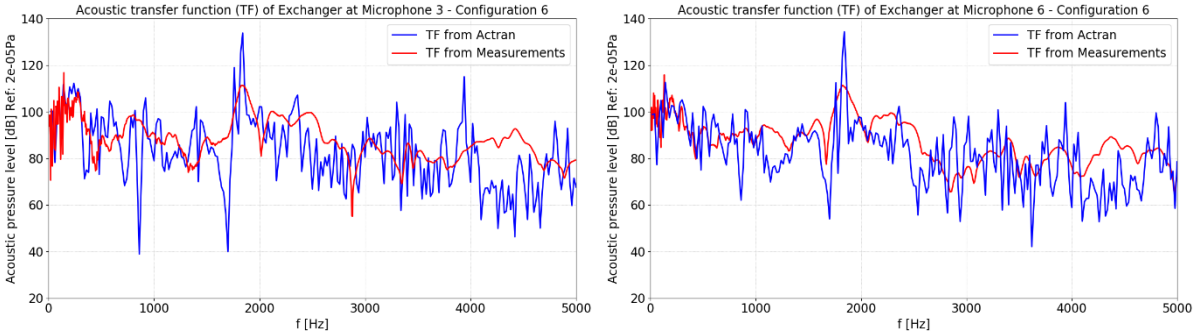


*Figure 15 - Acoustic transfer functions of exchanger with optimal Resistivity - Configuration 6*

The Figure 15 shows that the resistivity values found are also acceptable for another experimental configuration validating the numerical modelling of the heat exchanger. The existing gaps between the simulated and measured pressure results can be explained by the differences between the Actran model and the experimental set-up such as the assumption in the numerical model of an infinitely rigid structure of the module.

## 4. CONCLUSIONS

The present paper is dedicated to a noise analysis of a ventilation system. The analysis focused on the heat exchanger component which may reduce the noise level if located downstream the noise source. A numerical model including the visco-thermal effects of the acoustic propagation in small channels is presented. This model proposes a double fluid equivalent model avoiding a complex representation of each heat exchanger channels. The parameters are defined partly by the geometrical properties and by experiments operated on the real heat exchanger.

The combined experimental/numerical approach leads to a reliable numerical model and understanding of the noise propagation mechanisms in the ventilation system. Beyond the studied configurations, the obtained heat exchanger model can be used in the design and optimization of future more silent ventilation systems.

## 5. ACKNOWLEDGEMENTS

The authors would like to acknowledge the Walloon Region for the financial support of the research presented here, as part of the Silenthalpic project (C7711).

## 6. REFERENCES

[1] Y.Le, Y.Shen and J.Xia, A diffractive study on the relation between finite baffle and loudspeaker measurement, J. Audio Eng. Soc. 59(12), 944-952 (2011).

[2] G.B.Stan, J.J.Embrechts and D.Archambeau, Comparison of different impulse response measurement techniques, J. Audio Eng. Soc. 50(4), 249-262 (2002).

[3] Free Field Technologies, Actran 19 User's guide: Vol2, 2018.

[4] Beltman, W. M. (1998). Viscothermal wave propagation including acousto-elastic interaction. Department of Mechanical Engineering, University of Twente.

[5] Sambuc, C., Lielens, G., & Coyette, J. P. (2014). Numerical modelling of visco-thermal acoustics using finite elements. In *Proceedings of the ISMA*.

[6] Lielens G., Brandstetter M., Talbot A. (2018). Acoustic modeling of a Diesel Particulate Filter using a double equivalent fluid homogenization approach. In *Proceedings of the DAGA Conference.*